Electronic Supplementary Material (ESI) for ChemComm.

Supplementary Information

The First Porphyrin-subphthalocyaninatoboron(III)-fused Hybrid with Unique Conformation and Intramolecular Charge Transfer Behavior

Yuehong Zhang,‡[a] Juwon Oh,‡[b] Kang Wang,‡[a] Dongju Shin,[b] Xiaopeng Zhan,[a] Yingting Zheng,[a] Dongho Kim*[b] and Jianzhuang Jiang*[a]

Caption of Content

NMR spectra. As shown in Fig. S1, satisfactory ^{1}H NMR spectrum was obtained for **1** in CD_2Cl_2. All the signals could be unambiguously assigned with the result as detailed in Table S1. As can be seen, the ^{1}H NMR spectrum of **1** exhibits two doublets and one singlet at δ = 8.70, 8.62, and 7.99 ppm due to the pyrrole protons, respectively. The singlet at δ = 7.75 ppm is attributed to the protons on the quinoxaline ring, while the two singlets at δ = 8.53 and 8.45 ppm are assigned to the α protons from SubPc moiety. The signals for the aromatic protons of 2,6-dimethylphenoxyl substituents from the SubPc moiety exhibited two singlets at δ = 7.36 and 7.29 ppm. Whereas the singlets observed at δ = 7.63 and 7.57 ppm were attributed to the protons of the *meso*-attached aryl groups on Por moiety. The aromatic proton signals from Por moiety were observed at δ = 7.29 ppm, which was overlapped with one SubPc aromatic proton singlet. The two singlets at δ = 2.91 and 2.60 ppm and the multiplet at δ = 1.93-1.80 ppm are assigned to the methyl protons on Por moiety, and the broad peak appearing at δ = 2.32 ppm is attributed to the methyl protons on SubPc moiety. In addition, the singlet at δ = -2.21 ppm is due to the inner pyrrole protons. The two triplets δ = 6.70 and 6.58 ppm are assigned to the meta- and para- protons on the coordinated phenoxy ring, respectively. The signals for ortho protons are overlapped by the signal of the residue solvent CH_2Cl_2 due to their close locations.[1] Satisfactory NMR spectrum was also obtained for the reference SubPc **2**, and the signals are assigned in a similar manner (Fig. S2 and Table S1).

IR spectra. The IR spectra of **1** and **2** were shown in Fig. S13. In addition to the bands associated with the aromatic SubPc and Por moieties such as the C-H wagging and torsion vibrations (*ca.*767 and 710 cm^{-1}), and the isoindole ring and the C=N aza group stretching vibrations (*ca.*1490, 1447, 1406 and 1380 cm^{-1}),[2] the bands observed at 2973, 2916, and 2851 cm^{-1} are assigned to the asymmetric and symmetric C-H stretching vibrations of the $-CH_3$ groups, while those at 1278-1279 and 1092 cm^{-1} are ascribed to the asymmetric and symmetric C-O-C stretching vibrations of the 2,6-dimethylphenoxy groups in the SubPc moiety.[3] A weak band due to the asymmetrical N-H stretching vibration of the pyrrole moieties was observed at *ca.* 3349 cm^{-1} for **1** (Fig. S13).

Experimental Section

General Remarks: Chlorobenzene was freshly distilled from CaH_2 under nitrogen. Column chromatography was carried out on silica gel (Merck, Kieselgel 60, 70-230 mesh) column and biobead (BIORAD S-X1, 200-400 mesh) with the indicated eluents. All other reagents and solvents were used as received. The compounds of 4,5-bis(2,6-dimethylphenoxy)phthalonitrile,[4] 5,10,15,20-tetrakis(2,4,6-trimethylphenyl)porphyrin (**3**),[5] 5,10,15,20-tetrakis(2,4,6-trimethylphenyl)-2',3'-di-cyanopyrazino[2,3-*β*]porphyrin (**4**),[6] and 2,3-dicyanoquinoxaline[7] were prepared according to the published procedure. NMR spectra were recorded on a Bruker DPX 400 spectrometer. Spectra were referenced internally using the residual solvent resonances relative to $SiMe_4$. Electronic absorption spectra were recorded on a Lambda 750 spectrophotometer. IR spectra were recorded as KBr pellets using a Bruker Tensor 37 spectrometer with 2 cm^{-1} resolution. MALDI-TOF mass spectra were taken on a Bruker BIFLEX III ultra-high resolution Fourier transform ion cyclotron resonance (FT-ICR) mass spectrometer with *α*-cyano-4-hydroxycinnamic acid as the matrix. HR (high resolution) mass spectra were recorded on Solar IX MALDI-FT-MS. Elemental analyses were performed on an Elementar Vavio El III elemental analyzer. Electrochemical measurements were carried out with a BAS CV-50W voltammetric analyzer. The cell comprised inlets for a glassy-carbon-disk working electrode with a diameter of 2.0 mm in diameter and a silver-ware counter electrode. The reference electrode was Ag^+/Ag (a solution of 0.01 M $AgNO_3$ and 0.1 M TBAP in acetonitrile), which was connected to the solution by a Luggin capillary whose tip was placed close to the working electrode. It was corrected for junction potentials by being referenced internally to the ferrocenium/ferrocene (Fc^+/Fc) couple [$E_{1/2}(Fc^+/Fc)$ = 0.501 V *vs.* SCE]. Typically, a 0.1 M solution of $[NBu_4][ClO_4]$ in CH_2Cl_2 containing 1 mM of sample was purged with nitrogen for 10 min, and then the voltammograms were recorded

at ambient temperature. The scan rate was 20 mV/s for the electrochemical measurement.

X-ray crystallographic analysis of 1. Single crystals of **1** suitable for X-ray diffraction analysis were grown by diffusing CH_3CN into the $CHCl_3$ solution of the Por-SubPc-fused hybrid **1**. Crystal data and details of data collection and structure refinement are given in Table S2. Data were collected on an Oxford Diffraction Gemini E system with $Cu_{K\alpha}$ radiation λ = 1.5418 Å at 120 K, using a ω scan mode with an increment of 1^o. Preliminary unit cell parameters were obtained from 30 frames. Final unit cell parameters were obtained by global refinements of reflections obtained from integration of all the frame data. The collected frames were integrated using the preliminary cell-orientation matrix. The SMART software was used for data collecting and processing; ABSpack for absorption correction;[8] and SHELXL for space group and structure determination, refinements, graphics, and structure reporting.[9] CCDC-1477369 contains the supplementary crystallographic data for this paper. In this structure, the unit cell includes a large region of disordered solvent molecules, which could not be modelled as discrete atomic sites. We employed PLATON/SQUEEZE to calculate the diffraction contribution of the solvent molecules and, thereby, to produce a set of solvent-free diffraction intensities. For this structure, the SQUEEZE calculations showed a total solvent accessible area volume of 3368 $Å^3$ and the residual electron density amounted to 732 electron per unit cell, corresponding to nearly 12 molecules of $CHCl_3$ and 2 molecules of CH_3CN (about 3 $CHCl_3$ and 0.5 CH_3CN molecules per asymmetric unit). These data can be obtained free of charge from the Cambridge Crystallographic Data Centre via www.ccdc.cam.ac.uk/data_request/cif.

Density functional theory (DFT) and time-dependent density functional theory (TDDFT) calculations. The DFT method of HCTH147/6-311g(d) was used to calculate

the electronic structures of **1**-**2**. All the calculations were carried out by using the Gaussian 09 (Revision D.01) program.[10]

Steady-state Emission Measurements. Steady-state fluorescence spectra were measured on a Hitachi model F-2500 fluorescence spectrophotometer and a Scinco model FS-2. For the observation of steady-state emission spectra in near-infrared (NIR) region, a photomultiplier tube (Hamamatsu, R5108), a lock-in amplifier (EG&G, 5210) combined with a chopper and a CW He-Cd laser (Melles Griot, Omnichrome 74) for the 442 nm excitation were used.

Picosecond Time-resolved Fluorescence Measurements. Time-resolved fluorescence lifetime experiments were performed by the time-correlated single-photon-counting (TCSPC) technique. As an excitation light source, we used a Ti:sapphire laser (Mai Tai BB, Spectra-Physics) which provides a repetition rate of 800 kHz with ~ 100 fs pulses generated by a homemade pulse-picker. The output pulse of the laser was frequency-doubled by a 1 mm thickness of a second harmonic crystal (β-barium borate, BBO, CASIX).The fluorescence was collected by a microchannel plate photomultiplier (MCP-PMT, Hamamatsu, R3809U-51) with a thermoelectric cooler (Hamamatsu, C4878) connected to a TCSPC board (Becker&Hickel SPC-130). The overall instrumental response function was about 25 ps (the full width at half maximum (fwhm)). A vertically polarized pump pulse by a Glan-laser polarizer was irradiated to samples, and a sheet polarizer, set at an angle complementary to the magic angle (54.7°), was placed in the fluorescence collection path to obtain polarization-independent fluorescence decays.

Femtosecond Transient Absorption Measurements. The femtosecond time-resolved transient absorption (fs-TA) spectrometer consisted of Optical Parametric Amplifiers

(Palitra, Quantronix) pumped by a Ti:sapphire regenerative amplifier system (Integra-C, Quantronix) operating at 1 kHz repetition rate and an optical detection system. The generated OPA pulses had a pulse width of ~ 100 fs and an average power of 100 mW in the range 280-2700 nm which were used as pump pulses. White light continuum (WLC) probe pulses were generated using a sapphire window (3 mm of thickness) by focusing of small portion of the fundamental 800 nm pulses which was picked off by a quartz plate before entering to the OPA. The time delay between pump and probe beams was carefully controlled by making the pump beam travel along a variable optical delay (ILS250, Newport). Intensities of the spectrally dispersed WLC probe pulses are monitored by a High Speed spectrometer (Ultrafast Systems). To obtain the time-resolved transient absorption difference signal (ΔA) at a specific time, the pump pulses were chopped at 500 Hz and absorption spectra intensities were saved alternately with or without pump pulse. Typically, 4000 pulses excite samples to obtain the fs-TA spectra at a particular delay time. The polarization angle between pump and probe beam was set at the magic angle (54.7°) using a Glan-laser polarizer with a half-wave retarder in order to prevent polarization-dependent signals. Cross-correlation fwhm in pump-probe experiments was less than 200 fs and chirp of WLC probe pulses was measured to be 800 fs in the 400-800 nm region. To minimize chirp, all reflection optics in the probe beam path and the 2 mm path length of quartz cell were used. After the fluorescence and fs-TA experiments, we carefully checked absorption spectra of all compounds to detect if there were artifacts due to degradation and photo-oxidation of samples. HPLC grade solvents were used in all steady-state and time-resolved spectroscopic studies. The three-dimensional data sets of ΔA versus time and wavelength were subjected to singular value decomposition and global fitting to obtain the kinetic time constants and their associated spectra using Surface Xplorer software (Ultrafast Systems).

Preparation of the Por-SubPc-fused hybrid 1: To a mixed solution of 5,10,15,20-tetrakis(2,4,6-trimethylphenyl)-2',3'-dicyanopyrazino[2,3-*β*]porphyrin **4** (50.0 mg, 0.05 mmol) and 4,5-bis(2,6-dimethylphenoxy)phthalonitrile (250.0 mg, 0.68 mmol) in chlorobenzene (4.0 mL), a solution of boron trichloride (1.0 M in heptane, 1.5 mL, 2 equiv) was added at room temperature under nitrogen. The resultant mixture was heated to reflux under nitrogen for 4 h. After a brief cooling, the solvent was removed under reduced pressure and an excess amount of phenol (140.8 mg, 1.6 mmol) was added. The resulting mixture was heated at 130°C for 2 h. After removing the solvent under reduced pressure, the residue was chromotographed on a silica gel column with $CHCl_3$ as the eluent. The target products were further purified by biobead column chromatography with $CHCl_3$ as the eluent, giving the hybrid complex **1** as the first elution, followed by the symmetrical SubPc phenoxy-[2,3,9,10,16,17-hexakis(2,6-dimethylphenoxy)subphthalocyaninato]boron(III). Repeated chromatography followed by recrystallization from $CHCl_3$ and CH_3OH gave **1** (3.3 mg, 3.5%) as green powder. ^{1}H NMR (CD_2Cl_2, 400 MHz): δ 8.70 (d, 2H, J = 4 Hz), 8.62 (d, 2H, J = 4Hz), 8.53 (s, 2 H), 8.45 (s, 2 H), 7.99 (s, 2 H), 7.75 (s, 2 H), 7.63 (s, 2 H), 7.57 (s, 2 H), 7.36 (s, 6 H), 7.29 (s, 10 H), 6.70 (t, 2 H, J=8Hz), 6.58 (t, 1 H, J=8Hz), 5.30 (d, 2H), 2.91 (s, 6 H), 2.60 (s, 6 H), 2.32 (br, 24 H), 1.93-1.80 (m, 24 H), -2.21 (s, 2 H); UV/Vis (CH_2Cl_2): λ_{max} (logε)= 283 (4.84), 410 (5.25), 436 (5.27), 495 (4.55), 576 (4.83), 609 (4.87), 638 (4.89), 682 nm (4.30); MALDI-TOF MS: an isotopic cluster peaking at *m/z* 1682.7625, Calcd. for $C_{112}H_{94}BN_{12}O_4$, [*M*-OPh]$^+$ 1682.7649; Anal. Calcd. For $C_{118}H_{99}BN_{12}O_5 \cdot 1.5CHCl_3 \cdot 2H_2O$: C, 72.09; H, 5.29; N, 8.44. found: C, 71.95; H, 5.44; N, 8.19.

Preparation of the reference SubPc 2: By employing the above-described procedure with the precursor 2,3-dicyanoquinoxaline instead of precursor **4** as the starting material,

reference SubPc **2** was isolated in the yield of 5.7%. ^{1}H NMR (CD_2Cl_2, 400 MHz): δ 8.54 (q, 2 H, *J*=4Hz), 8.02 (q, 2 H, *J*=4Hz), 7.83 (s, 2 H), 7.72 (s, 2 H), 7.28-7.27 (m, 12 H), 6.37 (t, 2 H, *J*=8Hz), 6.56 (t, 1 H, *J*=8Hz), 5.25(d, 2H, *J* = 8Hz), 2.26 (s, 24 H); ^{13}C NMR ($CDCl_3$, 100 MHz): δ 152.06, 150.80, 150.66, 150.52, 150.26, 149.95, 144.63, 142.72, 141.49, 131.24, 130.99, 130.71, 129.69, 129.57, 128.88, 126.50, 126.16, 126.02, 125.76, 121.28, 118.43, 106.37, 106.07, 29.66, 16.14, 16.09; UV/Vis (CH_2Cl_2): λ_{max} (logε)= 283 (4.84), 356 (4.52), 474 (4.17), 559 (4.56), 578 nm (4.55); MALDI-TOF MS: an isotopic cluster peaking at *m/z* 927.3582, Calcd. for $C_{58}H_{44}BN_8O_4$, [*M*-OPh]$^+$ 927.3583; Anal. Calcd. For $C_{64}H_{49}BN_8O_5 \cdot 3.5CHCl_3 \cdot 3H_2O$: C, 54.30; H, 3.95; N, 7.50. found: C, 54.17; H, 4.01; N, 7.56.

References

1 G. E. Morse, A. S. Paton, A. Lough and T. P. Bender, *Dalton Trans.*, 2010, **39**, 3915-3922.

2 (*a*) J. Jiang, M. Bao, L. Rintoul and D. P. Arnold, *Coord. Chem. Rev.*, 2006, **250**, 424-448 and references therein; (*b*) S. Dong, D. Qi, Y. Zhang, J. Jiang and Y. Bian, *Vib. Spectrosc.*, 2011, **56**, 245-249.

3 (*a*) H. Shang, H. Wang, W. Li and J. Jiang, *Vib. Spectrosc.*, 2013, **69**, 8-12; (*b*) Y. Zhang, W. Cao, K. Wang and J. Jiang, *Dalton Trans.*, 2014, **43**, 9152-9157.

4 S. Makarov, C. Litwinski, E. A. Ermilov, O. Suvorova, B. Röder and D. Wöhrle, *Chem. Eur. J.*, 2006, **12**, 1468-1474.

5 M. Y. Hyun, Y. D. Jo, J. H. Lee, H. G. Lee, H. M. Park, I. H. Hwang, K. B. Kim, S. J. Lee and C. Kim, *Chem. Eur. J.*, 2013, **19**, 1810-1818.

6 S. Zhao, M. G. P. M. S. Neves, A. C. Tomé, A. M. S. Silva, J. A. S. Cavaleiro, M. R. M. Domingues and A. J. F. Correia, *Tetrahedron Lett.*, 2005, **46**, 2189-2191.

7 O. V. Hordiyenko, I. V. Rudenko, I. A. Zamkova, O. V. Denisenko, A. V. Biitseva, A.

Arrault and A. A. Tolmachev, *Synthesis*, 2013, **45**, 3375-3382.

8 Blessing, R. H. *Acta Crystallogr.*, 1995, **A51**, 33-38.

9 *SHELXL Reference Manual*, Version 5.1; Bruker Analytical X-Ray Systems: Madison, WI, 1997.

10 Gaussian 09, Revision D.01, M. J. Frisch, G. W. Trucks, H. B. Schlegel, G. E. Scuseria, M. A. Robb, J. R. Cheeseman, G. Scalmani, V. Barone, B. Mennucci, G. A. Petersson, H. Nakatsuji, M. Caricato, X. Li, H. P. Hratchian, A. F. Izmaylov, J. Bloino, G. Zheng, J. L. Sonnenberg, M. Hada, M. Ehara, K. Toyota, R. Fukuda, J. Hasegawa, M. Ishida, T. Nakajima, Y. Honda, O. Kitao, H. Nakai, T. Vreven, J. A. Montgomery, Jr., J. E. Peralta, F. Ogliaro, M. Bearpark, J. J. Heyd, E. Brothers, K. N. Kudin, V. N. Staroverov, T. Keith, R. Kobayashi, J. Normand, K. Raghavachari, A. Rendell, J. C. Burant, S. S. Iyengar, J. Tomasi, M. Cossi, N. Rega, J. M. Millam, M. Klene, J. E. Knox, J. B. Cross, V. Bakken, C. Adamo, J. Jaramillo, R. Gomperts, R. E. Stratmann, O. Yazyev, A. J. Austin, R. Cammi, C. Pomelli, J. W. Ochterski, R. L. Martin, K. Morokuma, V. G. Zakrzewski, G. A. Voth, P. Salvador, J. J. Dannenberg, S. Dapprich, A. D. Daniels, O. Farkas, J. B. Foresman, J. V. Ortiz, J. Cioslowski, and D. J. Fox, Gaussian, Inc., Wallingford CT, 2013.

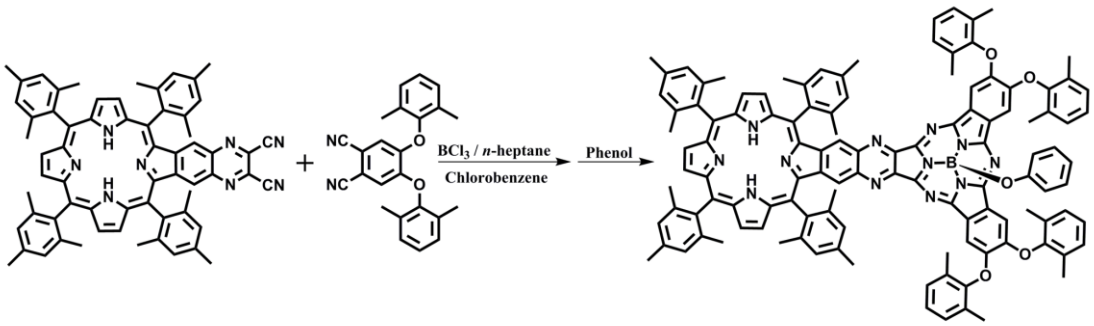

Scheme S1. Synthesis of Por-SubPc-fused hybrid **1**.

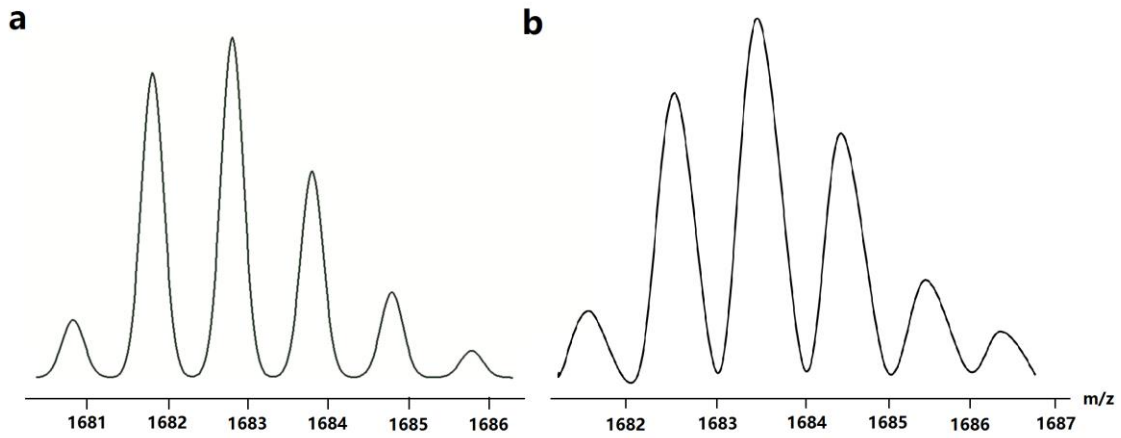

Fig. S1. Simulated (a) and experimental isotopic (b) pattern for the $[M\text{-OPh}]^+$ of Por-SubPc-fused hybrid (**1**).

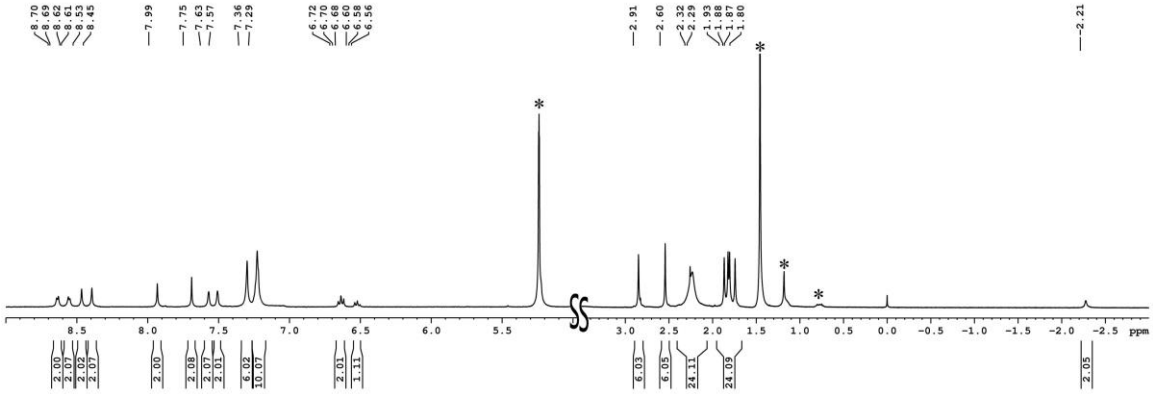

Fig. S2. ^{1}H NMR spectrum of **1** in CD_2Cl_2 at 298K; * indicates the signals for residual solvents.

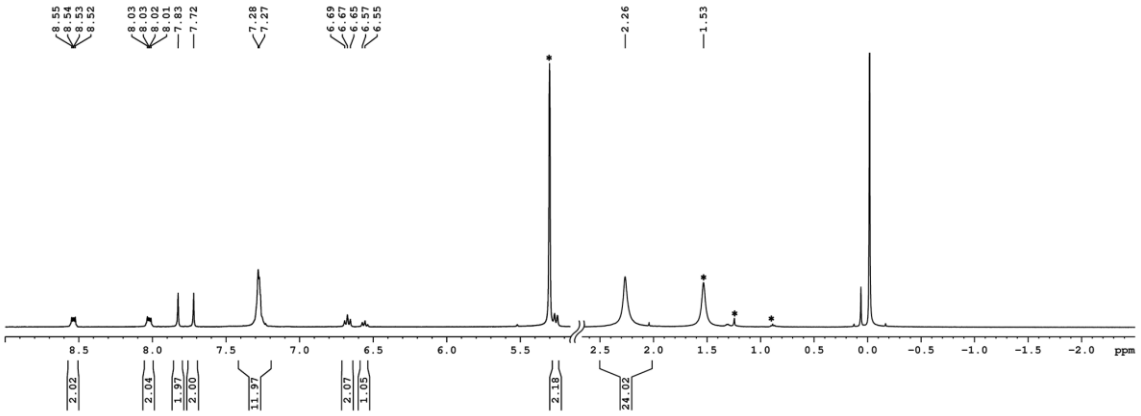

Fig. S3. ^{1}H NMR spectrum of compound **2** in CD_2Cl_2 at 298K; * indicates the signals for residual solvents.

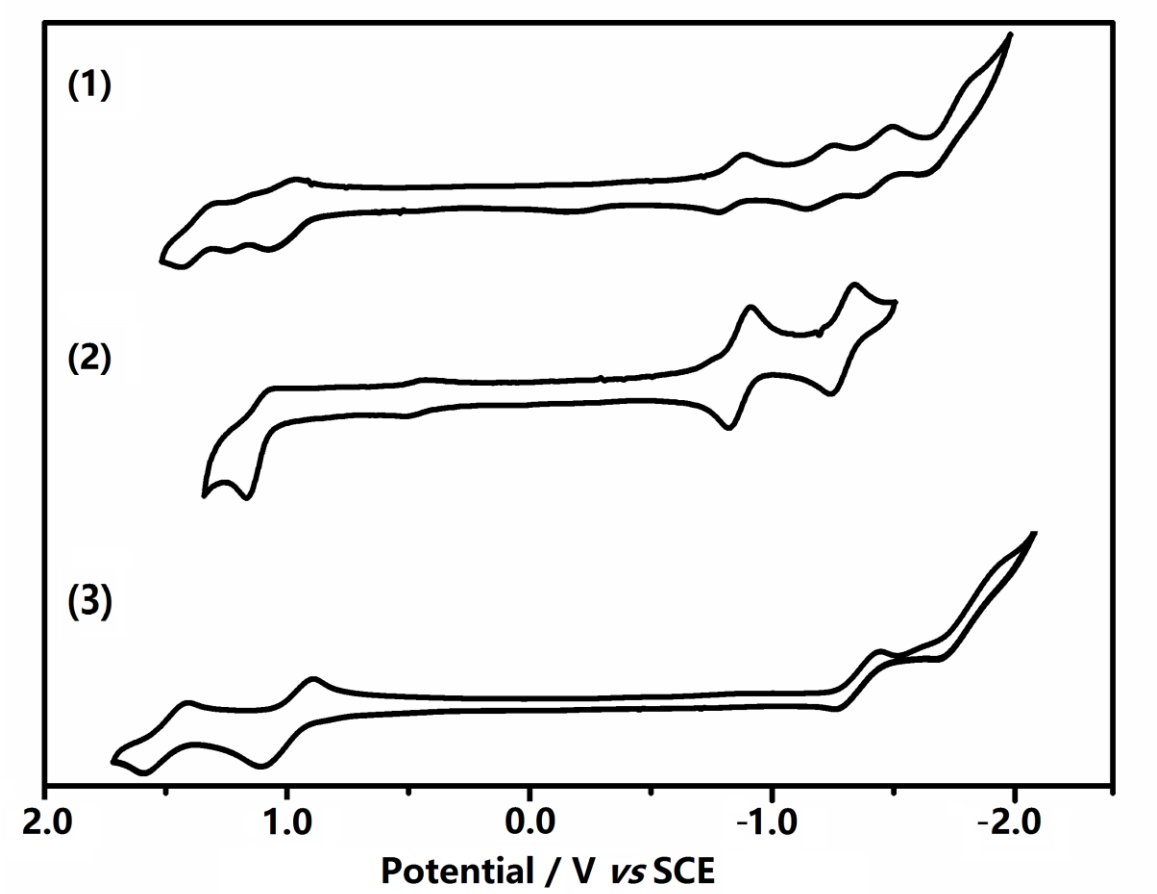

Fig. S4. Cyclic voltammograms of **1-3** in CH_2Cl_2 containing 0.1 mol·dm^{-3} $[Bu_4N]^+[ClO_4]^-$ at a scan rate of 20 mV·s^{-1} with Ag^+/Ag (a solution of 0.01 M $AgNO_3$ and 0.1 M TBAP in acetonitrile) as the reference electrode. It was corrected for junction potentials by being referenced internally to the ferrocenium/ferrocene (Fc^+/Fc) couple [$E_{1/2}(Fc^+/Fc)$ = 0.501 V *vs.* SCE].

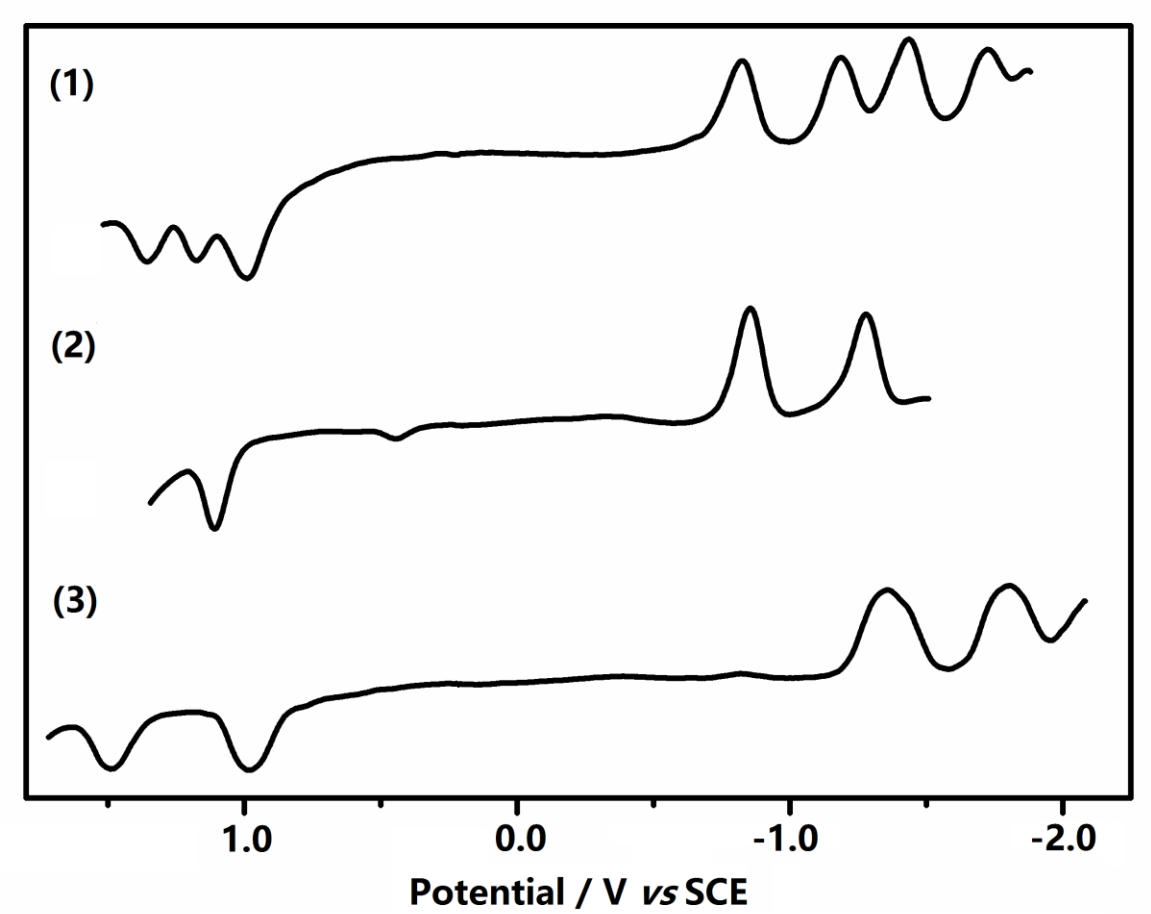

Fig. S5. Differential pulse voltammograms of **1-3** in CH_2Cl_2 containing 0.1 mol·dm^{-3} $[Bu_4N]^+[ClO_4]^-$ at a scan rate of 20 mV·s^{-1} with Ag^+/Ag (a solution of 0.01 M $AgNO_3$ and 0.1 M TBAP in acetonitrile) as the reference electrode. It was corrected for junction potentials by being referenced internally to the ferrocenium/ferrocene (Fc^+/Fc) couple [$E_{1/2}(Fc^+/Fc)$ = 0.501 V *vs.* SCE].

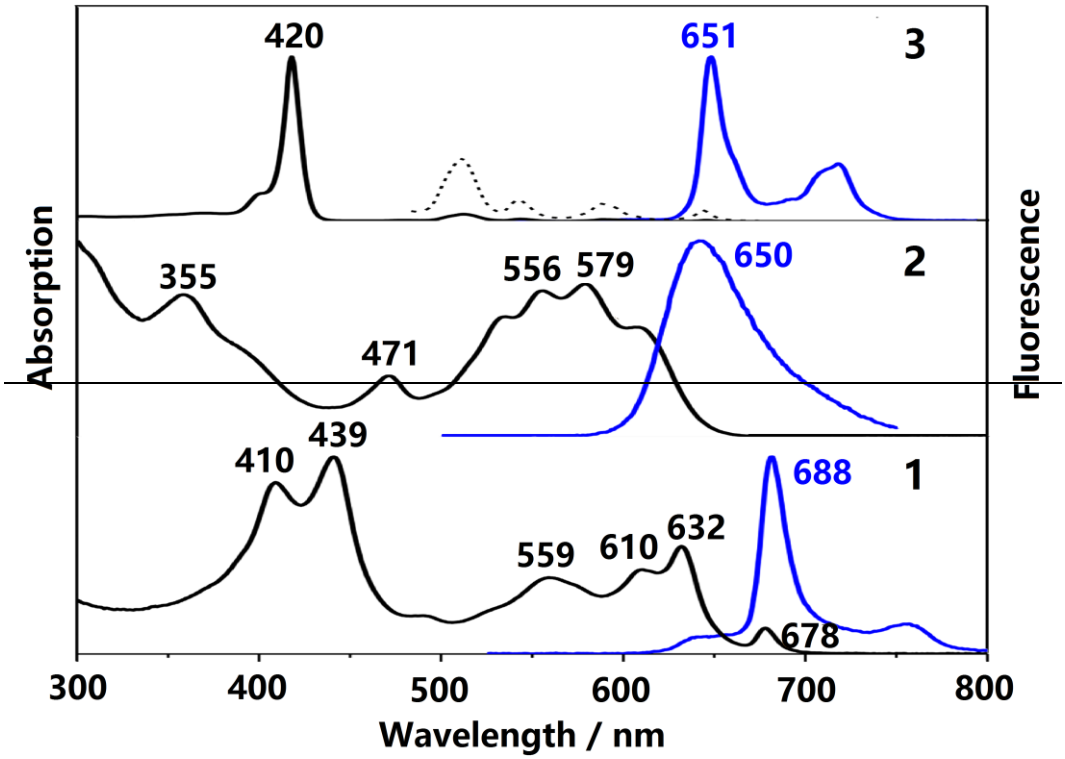

Fig. S6. Electronic absorption and fluorescence spectra for compounds **1**-**3** in toluene.

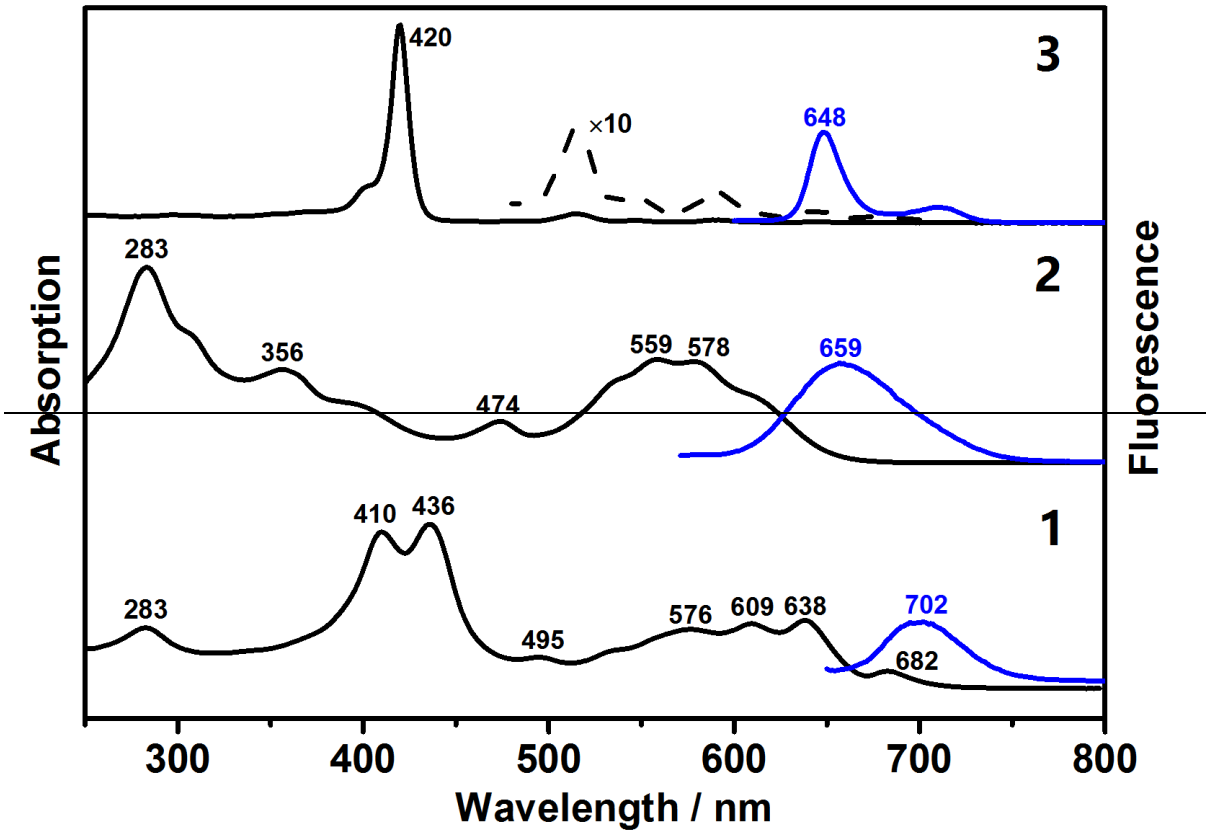

Fig. S7. Electronic absorption and fluorescence spectra for compounds **1**-**3** in CH_2Cl_2.

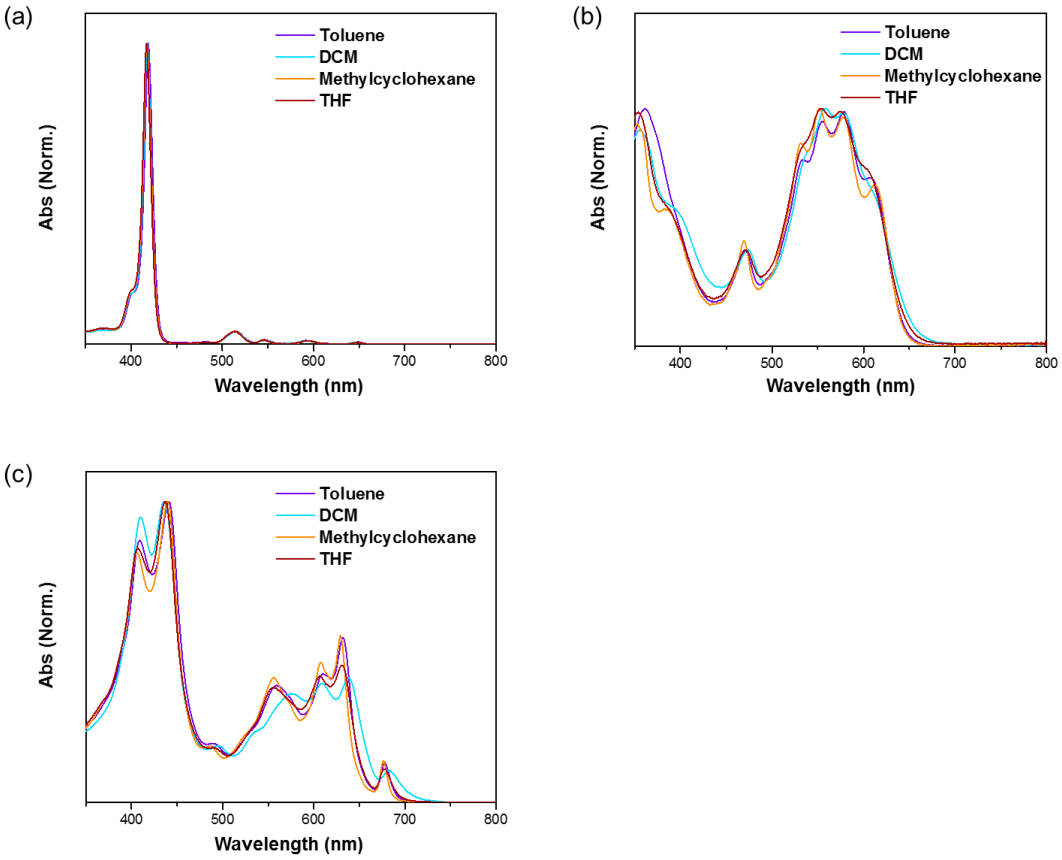

Fig. S8. Electronic absorption spectra of (a) **3,** (b) **2**, and (c) **1** in various solvents.

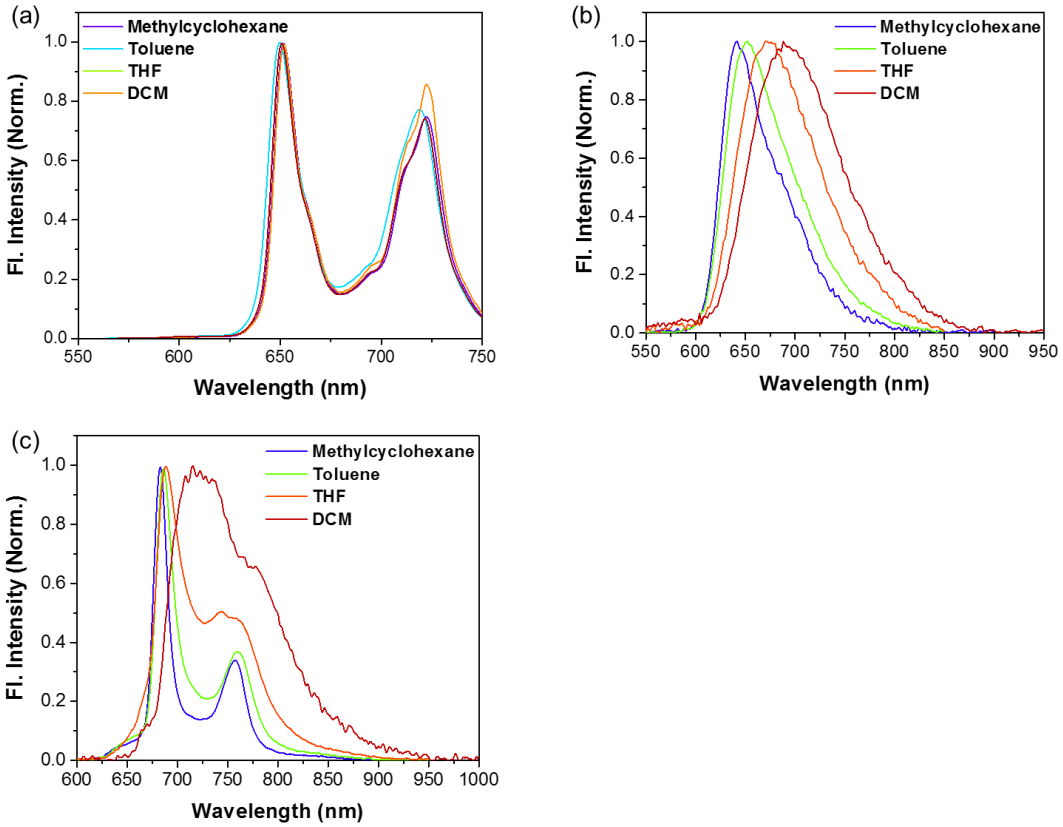

Fig. S9. Fluorescence spectra of (a) **3**, (b) **2**, and (c) **1** in various solvents.

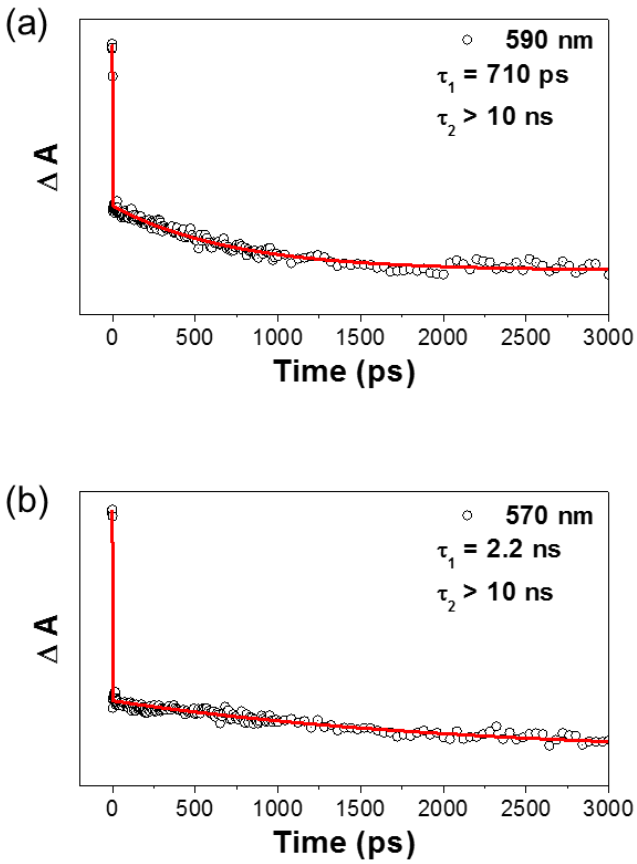

Fig. S10. fs-Transient absorption decay profiles for (a) **2** and (b) **1** with λ_{pump} = 600 nm in toluene at room temperature.

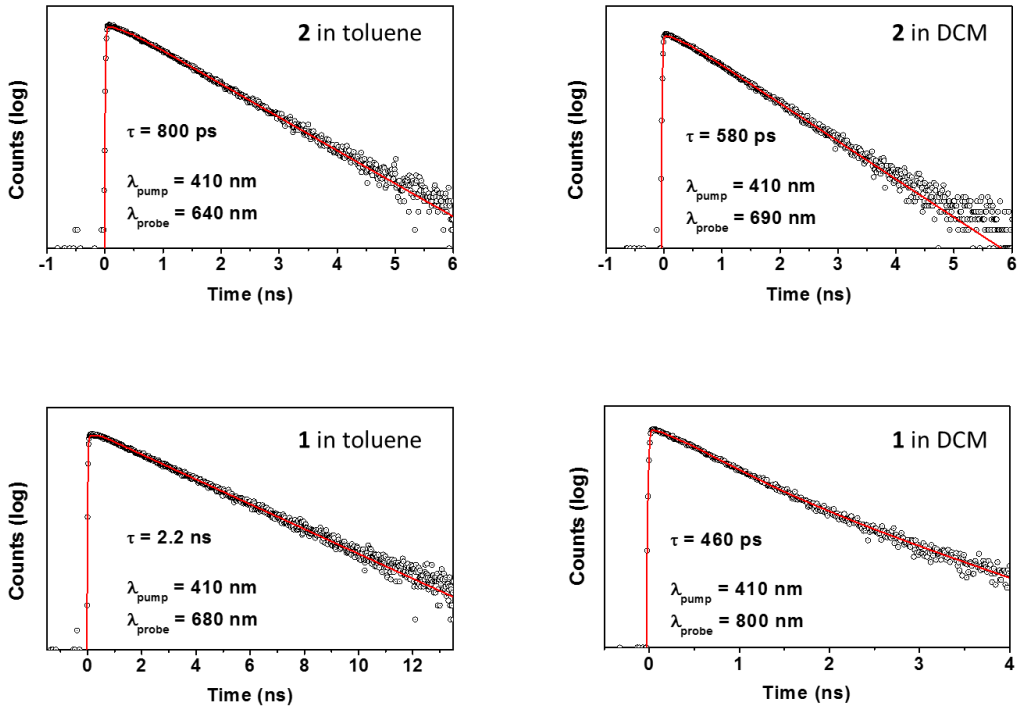

Fig. S11. Time-resolved fluorescence decay profiles for **1** and **2** in toluene and CH_2Cl_2.

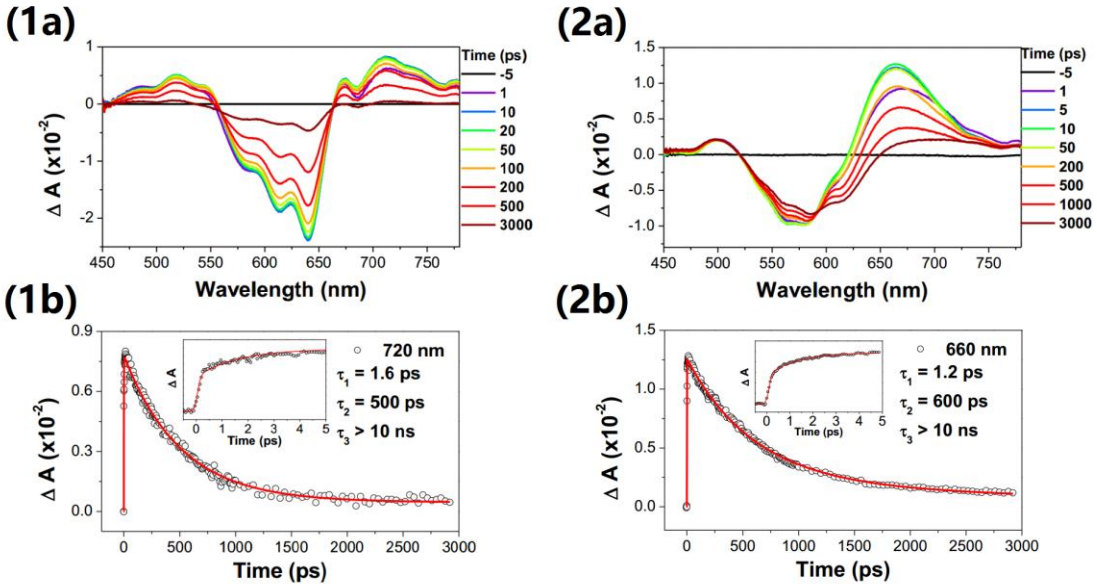

Fig. S12. fs-Transient absorption spectra (top) and decay profiles (bottom) for **1** (left) and **2** (right) with λ_{pump} = 600 nm in CH_2Cl_2 at room temperature.

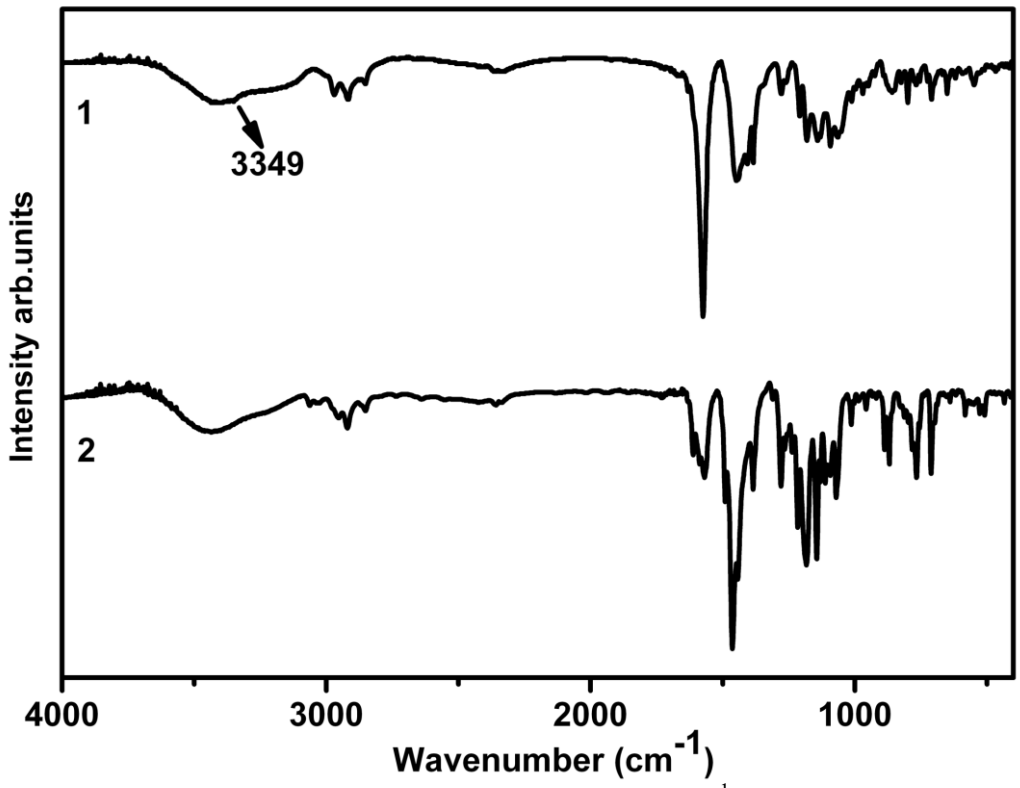

Fig. S13. IR spectra of **1** and **2** in the region of 400-4000 cm^{-1}.

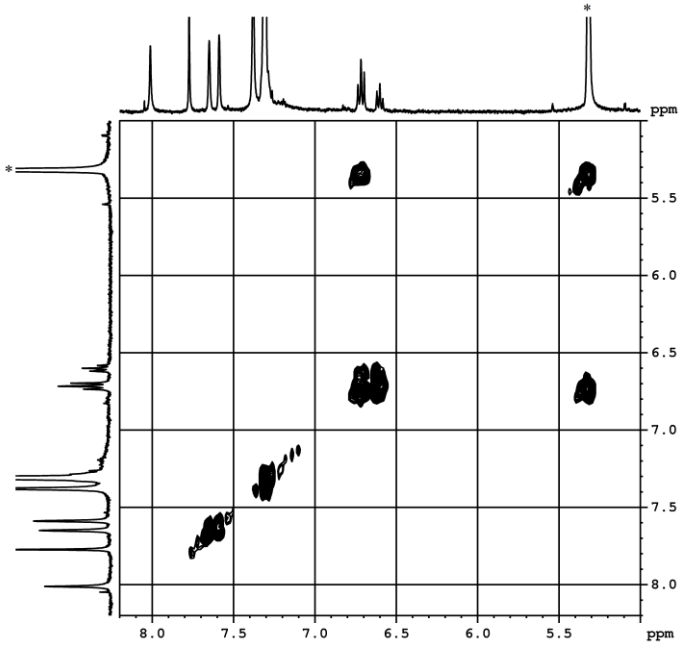

Fig. S14. ^{1}H-^{1}H COSY spectrum of **1** in CD_2Cl_2 at 298K; * indicates the signals for residual solvents.

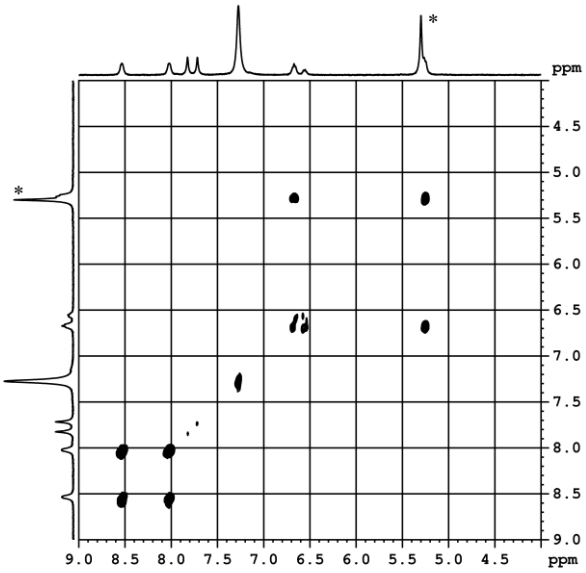

Fig. S15. ^{1}H-^{1}H COSY spectrum of **2** in CD_2Cl_2 at 298K; * indicates the signals for residual solvents.

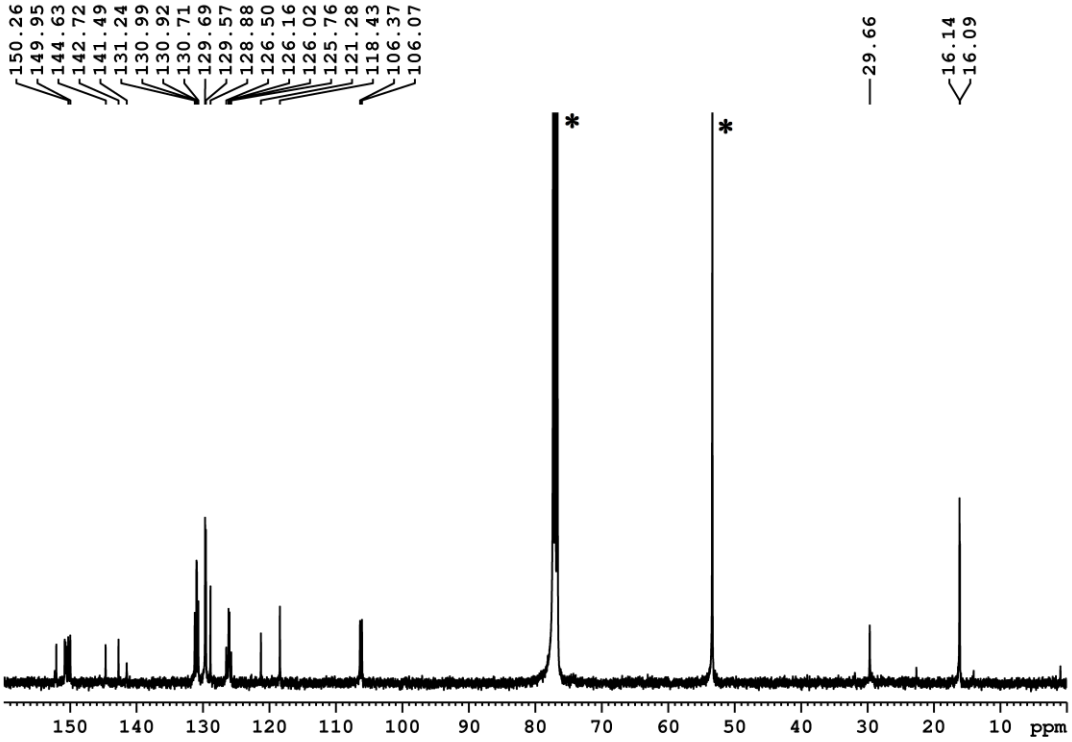

Fig. S16. ^{13}C NMR spectrum of **2** in $CDCl_3$ at 298K; * indicates the signals for residual solvents.

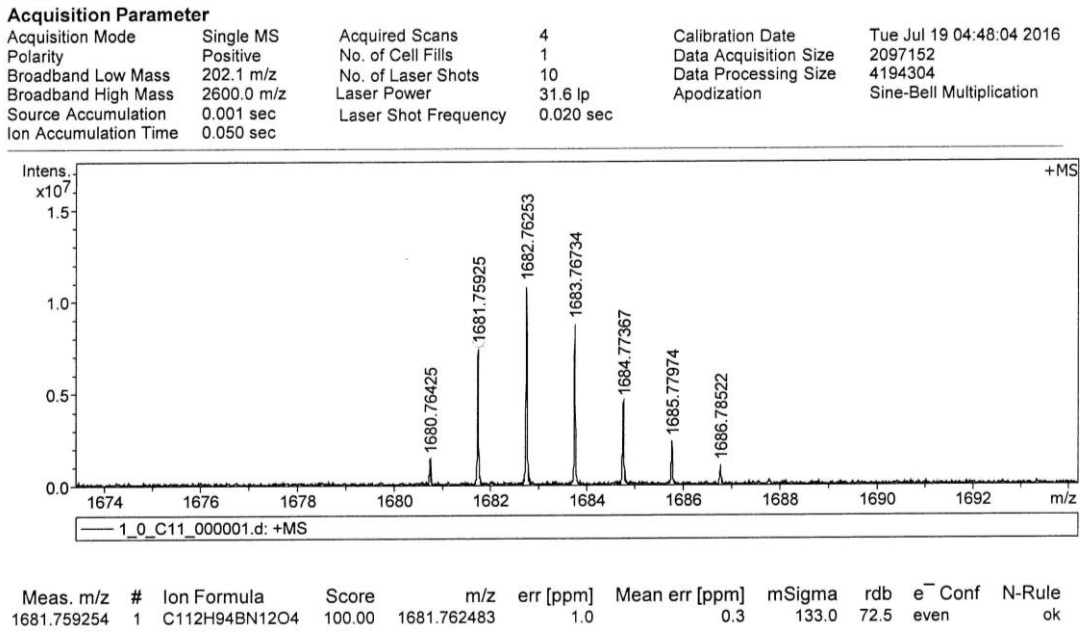

Fig. S17. HRMS for the Por-SubPc-fused hybrid (**1**).

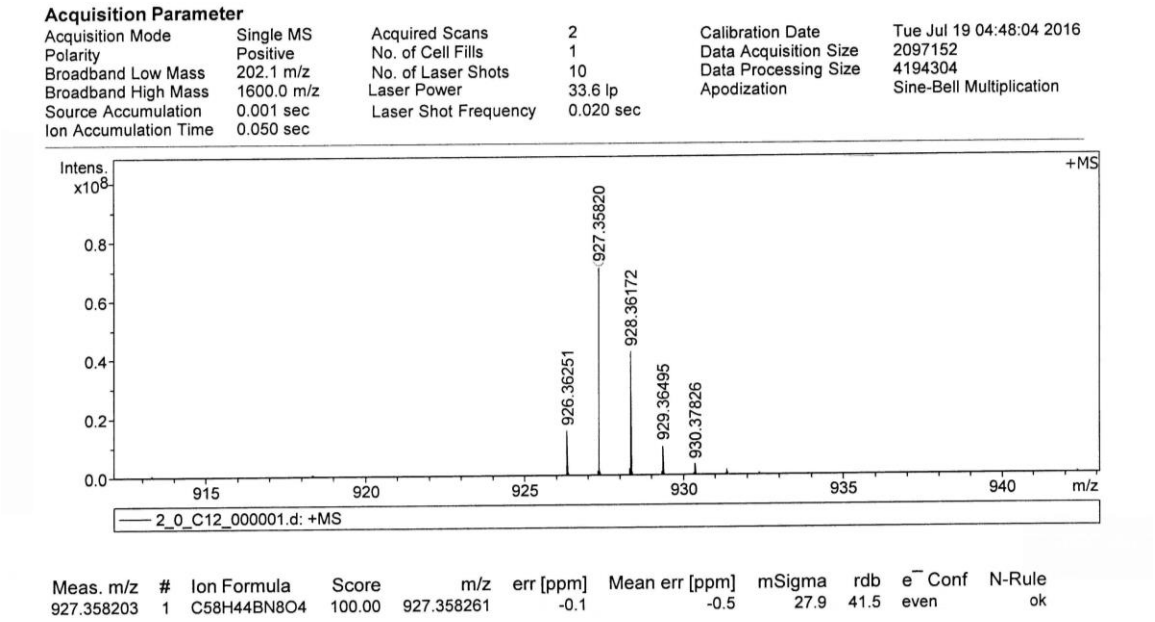

Fig. S18. HRMS for the SubPc (**2**).

Table S1. ^{1}H NMR data (δ) for the compounds **1-2** in CD_2Cl_2 at 298K.

Compound	SubPc				quinoxaline	Por			
	H_{α}	H_{aryl}	H_{OPh}	H_{methyl}		H_{β}	H_{aryl}	H_{methyl}	H_{NH}
1	8.53(s, 2 H), 8.45(s, 2 H)	7.29(s, 10H) [a], 7.36(s, 6H)	6.70(t, 2H, *J*=8Hz), 6.58(t, 1 H, *J*=8Hz), 5.30(d, 2H) [b]	2.32 (br, 24H)	7.75(s, 2 H)	8.70(d, 2 H, *J*=4Hz), 8.62(d, 2 H, *J*=4Hz), 7.99(s, 2 H)	7.29(s,10H) [a], 7.57(s, 2H), 7.63(s, 2H)	2.91 (s, 6H), 2.60 (s, 6H), 1.93-1.80(m, 24H)	-2.21(s, 2H)
2	7.83(s, 2 H), 7.72(s, 2H)	7.28-7.27(m, 12 H)	6.67(t, 2 H, *J*=8Hz), 6.55 (t, 1 H, *J*=8Hz), 5.25(d, 2H, *J*=8Hz)	2.26 (s, 24H)	8.54 (q, 2 H, *J*=4Hz), 8.02 (q, 2 H, *J*=4Hz)	--	--	--	--

[a] These protons signals were partially overlapped.

[b] The protons signals (doublet, 2H)were overlapped by the residual solvent CH_2Cl_2.

Table S2. Crystallographic data for the Por-SubPc-fused hybrid **1**.

	1[a]
Molecular formula	$C_{120}\ H_{101}\ B\ Cl_6\ N_{12}\ O_5$
M	2014.64
Crystal system	orthorhombic
Space group	$Cmc2_1$
a/Å	26.6592(9)
b/Å	23.6211(7)
c/Å	19.6982(7)
α/°	90
β/°	90
γ/°	90
U/Å^3	12404.4(7)
Z	4
D_c/Mg m^{-3}	1.079
μ/mm^{-1}	1.675
Data collection range/°	3.32 to 67.42
Reflections collected / unique	11919 / 6933 [R(int) = 0.0313]
Data/restraints/parameters	6933 / 43 / 607
R_1 [$I>2\sigma(I)$]	0.0831
wR_2 [$I>2\sigma(I)$]	0.2429
Goodness of fit	1.065

[a] In this structure, the unit cell includes a large region of disordered solvent molecules, which could not be modeled as discrete atomic sites. We employed PLATON/SQUEEZE to calculate the diffraction contribution of the solvent molecules and, thereby, to produce a set of solvent-free diffraction intensities. For this structure, the SQUEEZE calculations showed a total solvent accessible area volume of 3368 Å^3 and the residual electron density amounted to 732 electron per unit cell, corresponding to nearly 12 molecules of $CHCl_3$ and 2 molecules of CH_3CN (about 3 $CHCl_3$ and 0.5 CH_3CN molecules per asymmetric unit).

Table S3. Half-wave redox potentials of **1-3** recorded in CH_2Cl_2 containing 0.1 mol dm^{-3} $[Bu_4N][ClO_4]$ at a scan rate of 20 mV s^{-1}.[a]

Compound	Oxd_3[V]	Oxd_2[V]	Oxd_1[V]	Red_1[V]	Red_2[V]	Red_3[V]	Red_4[V]	$\Delta E^o_{1/2}$[V][b]
1	+1.35	+1.17	+0.99	-0.83	-1.19	-1.44	-1.72	1.82
2	--	--	+1.11	-0.86	-1.28	--	--	1.97
3	--	+1.49	+0.98	-1.36	-1.81	--	--	2.34

[a]Potentials are expressed as half-wave potentials ($E_{1/2}$) in V relative to SCE unless otherwise stated.
[b]$\Delta E^o_{1/2}$ is the potential difference between the first oxidation and first reduction processes.

Table S4. Electronic absorption data for **1** and **2** in toluene and CH_2Cl_2, respectively.

Compound /solvent	λ_{max}/nm (log ε)							
1/toluene	--	410 (5.13)	439 (5.24)	--	559 (4.74)	610 (4.78)	632 (4.87)	678 (4.26)
1/CH_2Cl_2	283 (4.84)	410 (5.25)	436 (5.27)	495 (4.55)	576 (4.83)	609 (4.87)	638 (4.89)	682 (4.30)
2/toluene	--	355 (4.35)	--	471 (3.77)	535 (4.05)	556 (4.13)	579 (4.15)	610 (4.01)
2/CH_2Cl_2	283 (4.84)	356 (4.52)	--	474 (4.17)	--	559 (4.56)	578 (4.55)	--

Table S5. Fluorescence quantum yields Φ_f and lifetime τ_f for the **1** and **2** in toluene and CH_2Cl_2, respectively.

Compound/solvent	Φ_f/%	τ_f/ps
1/toluene	7.3	2200
1/CH_2Cl_2	1	460
2/toluene	6	800
2/CH_2Cl_2	2	580